Competition on Nitrocellulose-immobilized Antibody Arrays

FROM BACTERIAL PROTEIN BINDING ASSAY TO PROTEIN PROFILING IN BREAST CANCER CELLS*

Garabet Yeretssian‡, Michèle Lecocq§, Guillaume Lebon§, Helen C. Hurst¶, and Vehary Sakanyan‡§‖

Large scale comparative evaluation of protein expression requires miniaturized techniques to provide sensitive and accurate measurements of the abundance of molecules present as individual and/or assembled protein complexes in cells. The principle of competition between target molecules for binding to arrayed antibodies has recently been proposed to assess differential expression of numerous proteins with one-color or two-color fluorescence detection methods. To establish the limiting factors and to validate the use of alternative detection for protein profiling, we performed competitive binding assays under different conditions. A model experimental protocol was developed whereby the competitive displacement of multi-subunit bacterial RNA polymerase and/or its subunits was evaluated through binding to subunit-specific immobilized monoclonal antibodies. We show that the difference in physico-chemical properties of unlabeled and labeled molecules significantly affects the performance of one-color detection, whereas epitope inaccessibility in the protein complex can prohibit the assessment of competition by both detection methods. Our data also demonstrate that antibody cross-reactivity, target protein truncation and abundance, as well as the cellular compartment of origin are major factors that affect protein profiling on antibody arrays. The experimental conditions established for prokaryotic proteins were adopted to compare protein profiles in the breast tumor-derived cell lines MDA MB-231 and SKBR3. Competitive displacement was detected and confirmed for a number of proteins using both detection methods; however, we show that overall the two-color method is better suited for accurate expression profile evaluation of a large, complex set of proteins. Antibody array data confirm the functional linkage between the ErbB2 receptor and AP-2 transcription factors in these cell lines and highlight unexpected differences in G_1 cyclin expression. ***Molecular & Cellular Proteomics 4:605–617, 2005.***

One of the great challenges in the field of post-genomic research is the large scale evaluation of protein expression in a variety of human pathologies, using miniaturized techniques to provide high sensitivity, short assay times, and minimal reagent consumption. Protein spots arranged in macroarray or microarray formats on planar supports are an attractive technique to use in this context, with the potential for high-throughput dissection of molecular interactions and the possibility of diversifying the array format to study a huge number of defined and/or noncharacterized proteins (1).

Many diseases are associated with, or even result from, modulations in protein expression. Therefore, monitoring simultaneously the expression profiles of a large number of proteins by antibody arrays can provide important information about the physiological status of the organism and can help to identify disease-specific biomarker candidates (2). Two main strategies have been proposed to compare and evaluate protein expression in cell lysates, both based on protein competition for binding to arrayed antibodies. The two-color approach detects differences in protein concentration between two cell lysates labeled by different fluorescent dyes and mixed in an equal ratio (3, 4). Two parallel experiments are run with mutually exchanged fluorescent dyes to reduce the possible interference from bio-conjugation bias of the dyes to proteins in the two samples. This method has been applied to evaluate protein profiling in human cancer cells and tissues (5–13). Recently a one-color approach (referred to as "competitive displacement") has been described that detects protein variations in lysates when the reference sample alone is labeled with a fluorescent dye (14, 15). Fluorescence intensity decreases differentially to be equivalent to, greater, or less than 50% displacement depending on the abundance of unlabeled proteins mixed in equal quantity with the labeled reference. This cost effective approach appears to be more convenient for large scale proteomic investigations. However, no data are available demonstrating the real competitiveness of labeled and unlabeled proteins on an antibody array, and it is important, therefore, to assess displacement activity in a single-protein competitive binding assay and to compare di-

From the ‡Biotechnologie, Biocatalyse, Biorégulation, Unité Mixte de Recherche 6204, Centre National de la Recherche Scientifique, Université de Nantes, 2 rue de la Houssinière, 44322 Nantes, France; §ProtNeteomix, Université de Nantes, 2 rue de la Houssinière, 44322 Nantes, France; and ¶Cancer Research UK Molecular Oncology Unit, Barts' and The London School of Medicine, London EC1M 6BQ, United Kingdom

Received, November 18, 2004, and in revised form, January 31, 2005

Published, MCP Papers in Press, February 2, 2005, DOI 10.1074/mcp.M400181-MCP200

rectly the performance of these two protein profiling detection methods.

In cells, many proteins are assembled into structural complexes in which a target epitope might be masked and thus not recognized by the corresponding antibody. To address this issue, we have used bacterial RNA polymerase (RNAP),[1] a complex protein model assembled via the dimerization of α subunits and the binding of β, β', ω, and one of the exchangeable σ subunits into a functionally active holoenzyme recognizing specific promoter sequences (16). To evaluate the one-color and two-color detection methods in protein profiling with antibodies arrayed on a nitrocellulose (NC) membrane, we have chosen near-infrared fluorescent dyes (IRDyes) for labeling proteins. Near-infrared fluorescence provides high sensitivity on membrane supports (17) and has been successfully used to detect molecular interactions on arrayed purified proteins (18), phage-displayed peptides (19), rat neuronal membrane fractions (20), and crude prokaryotic extracts (21). As the *Escherichia coli* α subunit of RNAP (αRNAP), labeled by IRDye, retains its binding ability to arrayed transcriptional factors (21), it has been used as a reporter to assess the competitiveness of labeled and unlabeled molecules in binding assays.

The information acquired from competition between individual prokaryotic proteins (RNAP and its subunits) has been used to compare more complex protein expression profiles in breast tumor-derived MDA MB-231 and SKBR3 cell lines with the aim of gaining insight into the functional grouping of targets involved in regulatory pathways. The data obtained with both detection methods were concordant for a few proteins; however, two-color detection allowed the abundance of a greater number of target proteins to be assessed, and we therefore conclude that this technique is better suited to high throughput protein profiling.

EXPERIMENTAL PROCEDURES

Affinity Purification of Tagged Proteins—The plasmid pET rpoA-his carrying the *E. coli* gene *rpoA* coding for αRNAP with a C-terminal His tag has been described previously (21). The recombinant protein was purified from *E. coli* BL21Star (DE3) (pET rpoA-his) cells grown in Luria-Bertani (LB) medium after induction with 1 mM isopropyl-1-β-D-thio-1-galactopyranoside (IPTG) at 37 °C for 5 h on a nickel-nitrilotriacetic acid (Ni-NTA) column according to the manufacturer's recommendations (Qiagen, CourtaBœuf, France). To express simultaneously the *E. coli* RNA polymerase α, β, β', and ω subunits and to purify the whole protein complex, we used a duet expression system composed of two compatible pET duet1 and pACYC duet1 vectors (Novagen, Fontenay-sous-bois, France) carrying respectively cloned his-rpoA, rpoB and rpoC, rpoZ genes. Details of the construction of pET duet1 his-rpoA, rpoB/pACYC duet1 rpoC, rpoZ and the purification of RNAP will be presented elsewhere.[2] The purified RNAP was compared with a commercial preparation (Epicenter, Madison, WI): protein purity was ascertained on a 12% SDS-PAGE followed by densitometry analysis.

Preparation of Bacterial Lysates for Competition Experiments—Recombinant *E. coli* BL21Star (DE3) strain (Invitrogen), carrying the plasmids pET rpoA-his or pET duet1 his-rpoA, rpoB/pACYC duet1 rpoC, rpoZ, were grown in LB medium to an OD_{600} of 0.6–0.8 and induced with 1 mM IPTG for up to 5 h. Aliquots were taken at 0, 1, 2, and 5 h of incubation, harvested by centrifugation, and resuspended in lysis buffer containing 50 mM NaH_2PO4 pH 8.0, 300 mM NaCl, 10 mM imidazole, 1 mg/ml lyzozyme. The cells, after incubation at 4 °C for 2 h, were sonicated and cleared by centrifugation. The supernatant was filtered through 0.2-μm hydrophilic sterile filters (Fisher Labosi, Elancourt, France). This step significantly reduced fluorescent "noise" during subsequent assays on NC membrane-immobilized antibody arrays. Total protein concentration was measured by a biophotometer (Eppendorf, Le Pecq, France) using the bicinchoninic acid method (22) or the Bradford method (23) with BSA as the calibration standard. If necessary, the lysates were labeled and used to assess competition of respective proteins under different experimental conditions (see "Results").

Preparation of Eukaryotic Lysates for Competition Experiments—Human breast carcinoma cell lines MDA MB-231 and SKBR3 were grown in Dulbecco's modified Eagle's medium with 4.5 g/liter glucose and L-glutamine (BioWhittaker, Verviers, Belgium) containing 10% FBS (BioMedia, Boussens, France) and 11.2 units/liter penicillin/11.2 μg/liter streptomycin at 37 °C and 5% CO_2. Cells were washed three times with PBS (137 mM NaCl, 2.7 mM KCl, 4.3 mM Na_2HPO_4 pH 7.4) and lysed in PBS with 1% Nonidet P-40 and 1× protease inhibitor mixture at 4 °C for 15 min. Cellular DNA was sheared by brief sonication, and the solubilized proteins were harvested by centrifugation at 13,000 rpm for 15 min. Subcellular Proteome Extraction kit (Calbiochem) was also used to recover a higher proportion of nondenatured target proteins from various cellular compartments. The yield and quality of partial proteomes corresponding to cytosolic, membrane/organelle, nucleus, and cytoskeleton proteins were verified by SDS-PAGE analysis according to the manufacturer's recommendations. Protein concentration was determined as described above.

Labeling Purified and Total Proteins in Cell Lysates with IRDyes—Purified proteins and prokaryotic or eukaryotic lysates were labeled with Alexa Fluor 680 (Molecular Probes, Cergy Pontoise, France) and/or IRDye 800CW (LiCOR Biosciences, Lincoln, NE) using a protocol adopted from Molecular Probes. Briefly, 5 μl of freshly prepared 1 M sodium bicarbonate buffer pH 8.3 was added to 50 μl of 2 mg/ml protein solution with the corresponding fluorescent dye, then incubated in the dark for 1 h with gentle shaking. The conjugated dye-protein complex was separated from free dye by gel filtration and eluted with PBS buffer. The average number of conjugated dye molecules was estimated, and samples with a final molar ratio of 2–3 dye molecules to 1 protein molecule were used to evaluate protein competitiveness in binding assays. Protein concentration was determined with a biophotometer as described above.

Western Blotting—Ten micrograms of total protein of prokaryotic cell extracts or 40 μg of total protein of eukaryotic cell extracts were separated on 12% SDS-PAGE and transferred to NC membrane. After blocking with PBS/0.05% Tween 20/5% skimmed milk, the membrane was incubated with the corresponding monoclonal pri-

[1] The abbreviations used are: RNAP, RNA polymerase; AP-2, activator protein-2; Cdk, cyclin-dependent kinase; ERK1, extracellular signal-regulated kinase 1; IgG, immunoglobulin G; IPTG, isopropyl-1-β-D-thio-1-galactopyranoside; IRDye, near-infrared fluorescence dye; JNK1/2, c-Jun N-terminal kinase 1/2; LB medium, Luria-Bertani medium; mAb, monoclonal antibody; MDM2, mouse double minute 2 protein; NC, nitrocellulose; NHS, *N*-hydroxysuccinimide; Ni-NTA, nickel-nitrilotriacetic acid; NMRAT, normalized ratio; pAb, polyclonal antibody; Rb, retinoblastoma; VEGF, vascular endothelial growth factor.

[2] G. Lebon, F. Marc, and V. Sakanyan, manuscript in preparation.

mary antibody in PBS/0.05% Tween 20/3% BSA at room temperature for 2 h. After washing in PBS/0.05% Tween 20, the membrane was incubated for 1 h with Alexa Fluor 680 goat anti-mouse IgG secondary antibody or IRDye 800-conjugated affinity-purified goat anti-rabbit IgG (LiCOR Biosciences). Fluorescent detection was achieved by scanning the membranes at 700 or 800 nm using the Odyssey Infrared Imaging system (LiCOR Biosciences). The fluorescent protein bands were quantified by Molecular Analyst (Bio-Rad Laboratories).

Preparation of Antibody Arrays—Both monoclonal (mAb) and polyclonal antibodies (pAb) against selected proteins were used to fabricate several designs of arrays with different sets of antibodies depending on the experimental purpose. The mAbs generated against *E. coli* RNA polymerase subunits α (mAb clone 4RA2), β (mAb clone NT63), and β' (mAb clone NT73) were purchased from NeoClone Biotechnology International (Madison, WI). Antibodies against eukaryotic proteins involved in stress response, cell-cycle progression, oncogenesis, apoptosis, and metastases were purchased from Interchim (Montlucon, France), BD PharMingen (San Diego, CA), Sigma-Aldrich (Lyon, France), and VWR International (Fontenay sous Bois, France). AP-2α (clone 8G8) and AP-2γ (clone 6E4) mAbs were described previously (24). Antibodies were serially 2-fold titrated within a range of 1–0.125 mg/ml and printed on glass slides covered in-house with Protran BA83 NC sheet or on commercial FAST™ slides (Schleicher & Schuell, Equevilly, France) using a manual microarray system (Microcaster, Schleicher & Schuell, Equevilly, France).

Binding Assays—Two methods were used to evaluate protein binding to NC-immobilized antibodies. To assess competitive displacement by one-color detection (14), the arrayed membranes were blocked prior to use in PBS containing 0.1–2% Tween 20 by slow agitation on a platform rocker at room temperature for 1 h. The blocking solution was discarded and membranes were then incubated with a labeled probe (usually at 1 μg/ml concentration) or with a mixture of labeled and unlabeled protein samples. If necessary, a competitive unlabeled sample (as purified protein or total protein in lysates) was added at increasing ratios corresponding to 1, 10, or 100 μg/ml of total protein concentration. Membranes were incubated at room temperature for 30 min, washed three times with high-salt PBS-T buffer (PBS containing 500 mM sodium chloride and 0.1% Tween 20), and then dried. Fluorescent signals were detected by scanning membranes with the Odyssey Infrared Imaging system (LiCOR Biosciences).

In two-color detection, antibody arrays were incubated with an equal mixture of samples labeled with IRDye 800CW and Alexa Fluor 680 under the conditions described above and washed using a Protein Array Workstation (PerkinElmer Life Sciences).

Data Acquisition and Statistical Analysis—The software GenePix Pro 4.0 (Axon Instruments, Union City, CA) was used to quantify the image data. The local background in the near-infrared fluorescent wavelength channel was subtracted from the fluorescent signal registered from each antibody spot. Only spots displaying a fluorescent intensity greater than twice the level of background noise were used for further analysis.

Mean values of quadruplicate readings were used for the analysis of fluorescent intensity from spots detected by the one-color method. The degree of competition between labeled and unlabeled samples displaced at a 1:1 ratio (the best statistical fit to monitor displacement), were subtracted from values obtained after competition between the same labeled reference and another unlabeled sample.

In the two-color evaluation, data were scaled such that the average mean ratio value for all of the spots on each separate array was normalized to 1, with the premise that the average spot on the chip would represent unchanged protein expression. A data-based criterion was determined, above or below which proteins were found to be differentially expressed. To determine such a cutoff level, a hierarchical model approach was used (4) in which the parameters were estimated using ANOVA.

Normalized ratio (NMRAT) values outside the interval of 0.72–1.28 were considered differentially expressed with 95% statistical confidence when analyzing *E. coli* cell extracts in imitation experiments. NMRAT values outside the interval of 0.83–1.17 and 0.73–1.27 were considered differentially expressed with, respectively, 70 and 90% statistical confidence when analyzing total protein lysates of breast cancer MDA MB-231 and SKBR3 cell lines. To analyze proteins derived from the nuclear subfraction of the same cell lines, NMRAT values outside the intervals 0.82–1.18 and 0.71–1.29 were considered differentially expressed with, respectively, 70 and 90% statistical confidence.

RESULTS

Rationale of the Protein Competition Assay on NC-immobilized Antibody Arrays—A general schema of the protocol used to assess single-protein competition on antibody arrays is shown in Fig. 1*B*. Epitopes of the *E. coli* RNA polymerase α, β, and β' subunits were used to follow the displacement of the purified αRNAP protein or the whole RNAP protein complex or the overexpressed proteins in crude extracts obtained from IPTG-induced cells.

Barry *et al.* used hydrogel-arrayed antibodies to carry out competitive displacement of proteins followed by one-color detection (14). We were concerned that such a support might differentially affect the penetration of labeled and unlabeled samples into the gel and therefore chose to print antibodies onto an NC membrane, which we have previously shown to be highly efficient in studying molecular interactions using IRDye-labeled probes (21).

A four-parameter logistic regression method (25), used for competitive binding immunoassays, was applied to construct a plot of signal intensity *versus* analyte concentration.

$$y = [(a - d)/1 + (x/c)^b] + d \quad \text{(Eq. 1)}$$

This shows the inverse relationship between the fluorescent signal y (fluorescence intensity at 700 or 800 nm) and the concentration of the unlabeled analyte x (protein in μg/ml) in which a is the maximum fluorescence estimated at zero concentration of x; b is the slope factor for the transition between a and d; c is the mid-range concentration of analyte corresponding to the point of inflection on the sigmoid; and d is the minimal signal at infinite x concentration corresponding to the background detected on an NC membrane. Signals can be normalized as a ratio of B and B_0 corresponding to two fluorescent signals calculated respectively as $a - d$ and $y - d$.

Assuming that no dissociation and rebinding occurs under the standardized conditions, the competition between labeled and unlabeled proteins for the single-antibody epitope should lead to 50, 90, and 99% displacement, respectively, at a mixed labeled:unlabeled sample ratio of 1:1, 1:10, and 1:100 as compared with the labeled reference protein or lysate. A typical competitive displacement curve for the purified bacterial αRNAP, displayed on a semi-log plot, shows that the diminution of the fluorescent signal intensity (% B/B_0) is de-

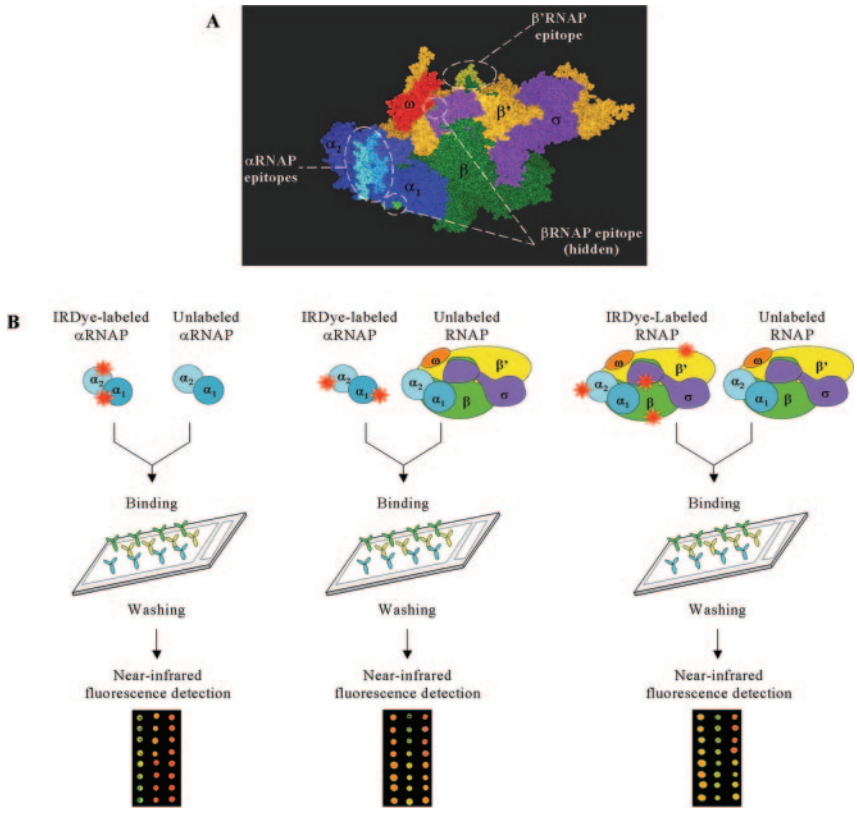

FIG. 1. **Schematic representation of the model protocol used to evaluate competitive displacement with one-color detection.** *A*, three-dimensional structure of the *T. thermophilus* RNA polymerase (PDB ID: 1IW7). Positions of the epitopes in the three RNAP subunits are *circled*. *B*, displacement experiments were performed with both purified proteins and crude cell extracts of appropriate recombinant *E. coli* strains. Competition by αRNAP and RNAP was evaluated both using labeled αRNAP and labeled RNAP (see "Results").

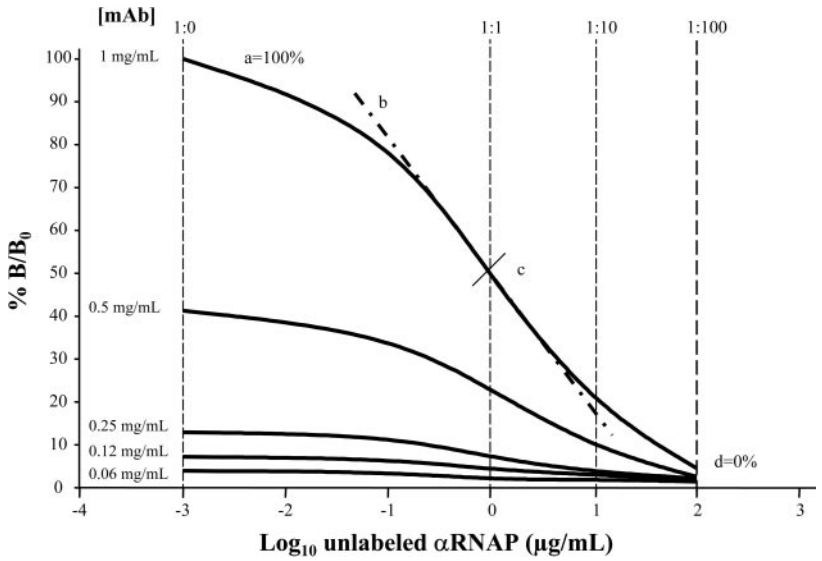

FIG. 2. **Typical displacement curves obtained for bacterial αRNAP in one-color detection.** Each curve corresponds to a given concentration (from 0.06 to 1 mg/ml) of immobilized anti-αRNAP antibody as indicated. Ratios of labeled:unlabeled proteins are shown at the *top* of the plot.

pendent on an increase in the unlabeled analyte concentration within a detectable concentration range of immobilized antibodies (Fig. 2). B/B_0 was plotted against the logarithm of the concentration of unlabeled αRNAP using Origin 7.0 software (OriginLab Corporation, Northampton, MA).

Competition between Purified αRNAP Molecules—In preliminary experiments, Alexa Fluor 680-labeled αRNAP, at concentrations ranging from 0.1 to 10 μg/ml in the binding solution, was incubated with anti-αRNAP mAb printed from 2-fold titrated antibody samples on a NC membrane. Increasing fluorescent background was observed at concentrations above 1 μg/ml; therefore, further measurements were performed at this concentration for all labeled analytes tested.

Next, the immobilized anti-αRNAP mAb (printed from 2-fold titrated solutions at concentrations ranging from 1 to 0.06

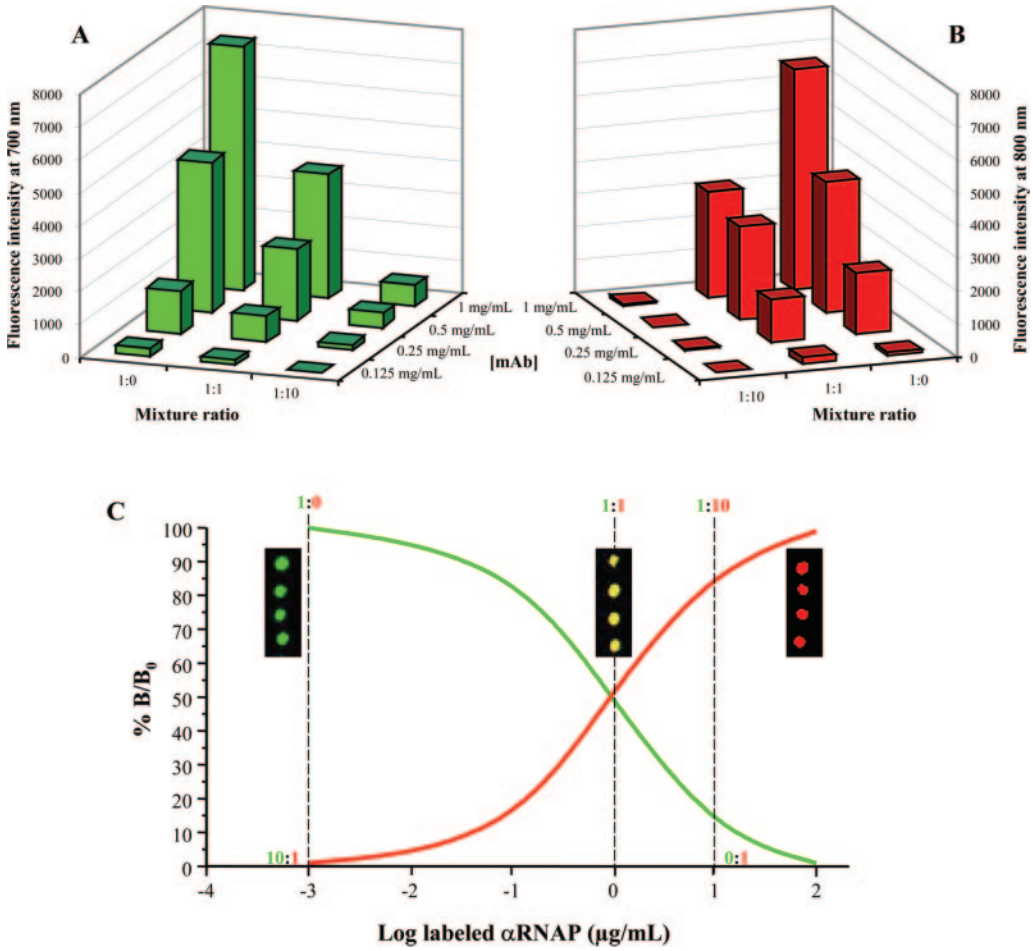

FIG. 3. **Assessment of the two-color detection method.** Histograms of competitive displacement assessed in a mixture of Alexa Fluor 680 (*A*) and IRDye 800CW (*B*) labeled αRNAP molecules. The same data are also displayed as displacement curves (*C*). Experiments were carried out using 12 replicates (four replicates on three slides) with an average standard deviation of 8.6%. Representative fluorescence spots are shown for each ratio.

mg/ml) was probed with labeled αRNAP alone or a mixture of labeled:unlabeled αRNAP at various ratios. A diminution in the fluorescent signal, close to the expected theoretical values, was detected from spots corresponding to anti-αRNAP from 1 and 0.5 mg/ml antibody dilutions (see Fig. 2). The signal was weaker and poorly interpretable from spots printed at antibody concentrations less than 0.25 mg/ml. Therefore, further measurements were done by taking into account only signal intensities detected on spots printed from 1 and 0.5 mg/ml antibody concentrations.

To evaluate the accuracy of the competition between αRNAP molecules, we took advantage of the two-color fluorescent detection method, enabling us to monitor the behavior of identical molecules labeled differentially. Purified αRNAP samples, separately labeled with Alexa Fluor 680 and IRDye 800CW, were mixed in different ratios and probed with the immobilized anti-αRNAP mAb. The reduction in fluorescent intensity at 700 nm (Fig. 3*A*) was accompanied by the appearance of a fluorescent signal at 800 nm (Fig. 3*B*). A good correlation in the modulation of the signal intensity confirmed the inverse relationship of the binding competition between two identical proteins, for the anti-αRNAP mAb arrayed on an NC membrane (Fig. 3*C*).

Competitive Displacement of αRNAP in Bacterial Cell Lysates—To assess the competitiveness of αRNAP in more complex bacterial cell extracts, we determined the displacement of this protein synthesized in *E. coli* BL21Star (DE3) (pET rpoA-his) cells, obtained after 1-h IPTG induction of the *rpoA* gene, using labeled sample mixed with the purified unlabeled protein. A strong, 75% diminution of the signal was detected after addition of an equal amount of purified αRNAP (data not shown) indicating that the concentration of the target protein was lower in the crude lysates than the concentration of the added protein. In contrast, when a mixture of labeled and unlabeled lysates of *E. coli* BL21Star (DE3) (pET rpoA-his) of 1-h induced cells was tested, the displacement was more reminiscent of that observed between purified αRNAP molecules (see Fig. 2).

Competition between αRNAP and the RNAP Complex—Next, we were interested in determining whether competition

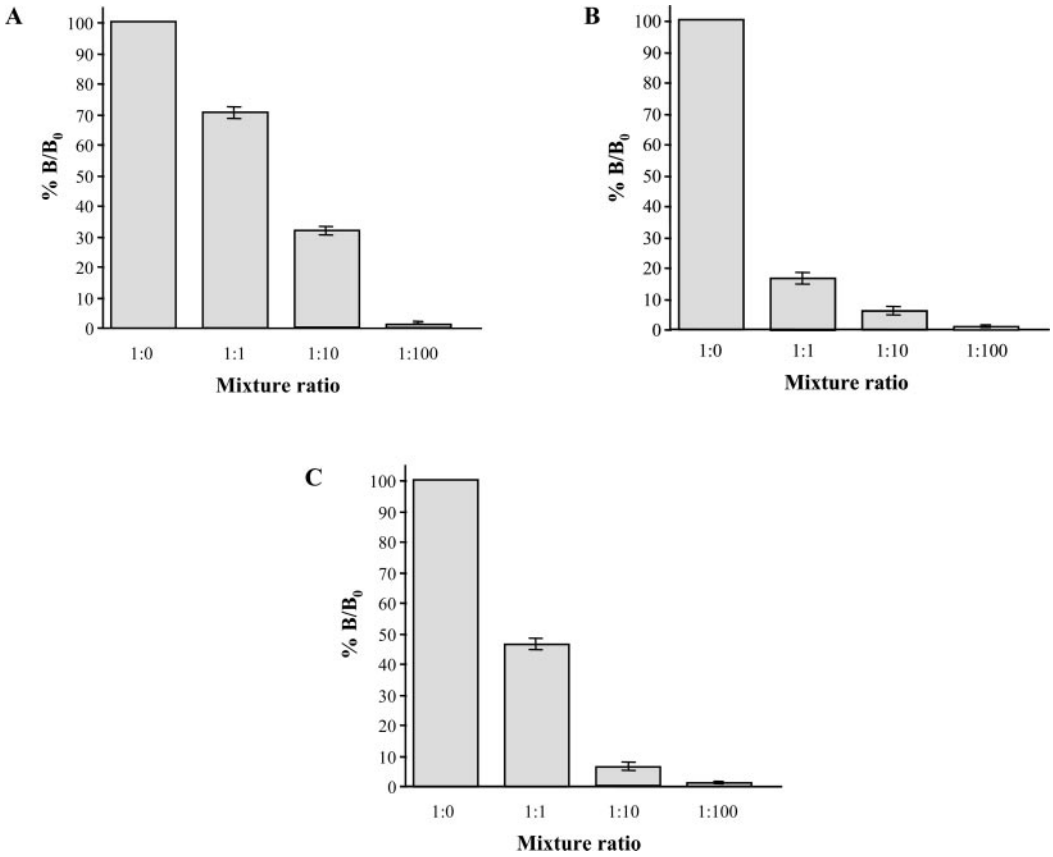

FIG. 4. **Competition between αRNAP and whole RNAP or between whole RNAP molecules.** Displacement between labeled lysate of 1-h-induced *E. coli* BL21Star (DE3) (pET rpoA-his) and unlabeled purified RNAP (*A*), labeled lysate of 1-h-induced *E. coli* BL21Star (DE3) (pET duet1 his-rpoA, rpoB/pACYC duet1 rpoC, rpoZ) and unlabeled purified αRNAP (*B*), or unlabeled purified RNAP (*C*).

occurs between small αRNAP and large RNAP molecules. A labeled lysate (1 μg/ml total protein) of the *E. coli* BL21Star (DE3) (pET rpoA-his) cells, induced with IPTG for 1 h, was competed with purified unlabeled RNAP. A clear diminution in fluorescence intensity was detected corresponding to 30 and 70% displacement of αRNAP, respectively, for 1:1 and 1:10 ratios (Fig. 4*A*). However, this displacement rate was weaker compared with the competition between individual αRNAP molecules (see the previous section).

To confirm the competitiveness of whole RNAP, we also tested lysate of *E. coli* BL21Star (DE3) (pET duet1 his-rpoA, rpoB/pACYC duet1 rpoC, rpoZ) cells, induced with IPTG for 1 h to allow simultaneous overexpression and assembly of α, β, β′, and ω subunits into a whole RNAP enzyme. Competition between the labeled lysate and the unlabeled purified αRNAP resulted in strong 85 and 95% displacement, respectively, at 1:1 and 1:10 ratios (Fig. 4*B*).

These data showed that αRNAP and the RNAP complex can compete for immobilized anti-αRNAP mAb. However, the large protein complex was less competitive compared with the smaller αRNAP molecule, and this can be explained, at least partially, by the lower molar presentation of the α-subunit in RNA polymerase.

Competitive Displacement of the RNAP Complex in Bacterial Cell Lysates—To gain insight into the competition behavior of a whole RNAP, we assessed its displacement in a mixture of labeled extract of *E. coli* BL21Star (DE3) (pET duet1 his-rpoA, rpoB/pACYC duet1 rpoC, rpoZ) cells after 1-h IPTG induction and in the unlabeled RNAP. The binding was followed in parallel assays with anti-αRNAP, anti-βRNAP, and anti-β′RNAP mAbs immobilized on the same NC membrane. As shown in Fig. 4*C*, 55 and 95% displacement of the labeled lysate by unlabeled RNAP was detected with the anti-αRNAP mAb, respectively, at 1:1 and 1:10 ratios. Low fluorescence was observed from anti-βRNAP and anti-β′RNAP mAb spots with and without addition of unlabeled RNAP, which indicated that no displacement occurred under the conditions used (data not shown).

Similar experiments were performed with labeled and unlabeled lysates from *E. coli* BL21Star (DE3) (pET duet1 his-rpoA, rpoB/pACYC duet1 rpoC, rpoZ) obtained from 1-h IPTG-induced cells. Again, displacement was clearly observed with the anti-αRNAP mAb, whereas no competition was detected with anti-βRNAP and anti-β′RNAP mAbs (data not shown).

To clarify this discrepancy in the competitive displacement, we followed the kinetics of α, β, and β′ subunit expression (as

soluble proteins in the supernatant) in IPTG-induced cells of *E. coli* BL21Star (DE3) (pET duet1 his-rpoA, rpoB/pACYC duet1 rpoC, rpoZ) using Western blotting. As shown in Fig. 5, an abundant band corresponding to each protein appeared after 1-h induction. Densitometry of these protein bands revealed that the yield of α, β, and β' subunits was, respectively, 11-, 6-, and 4-fold greater in 1-h-induced cells compared with noninduced ones. However, further induction of the cells up to 5 h resulted only in 1.3- and 1.8-fold further increases in the yield of αRNAP and β'RNAP, whereas the yield of βRNAP increased 1.6-fold after 2 h induction and thereafter decreased to the level of a 1-h induction.

Based on these data, we attempted to evaluate the competition between labeled lysates of 2- or 5-h-induced cells and the unlabeled RNAP. Again, the displacement was only detected from spots with immobilized anti-αRNAP mAb but not with anti-βRNAP and anti-β'RNAP mAbs (data not shown).

Imitation of Protein Profiling Using Crude Bacterial Lysates—We next asked whether the competitive displacement can be detected in lysates obtained from bacterial host cells in which whole polymerase or its α subunit were differentially expressed. To compare the amount of αRNAP synthesized in 1- and 2-h-induced cells, we mixed labeled and unlabeled lysates at 1:1 ratio and incubated the mixture with the arrayed anti-αRNAP mAb. The difference in protein expression deduced from the spots was found to be +25% when the labeled reference was the 1-h-induced lysate (Fig. 6*A*, compare the first two columns), whereas it was –15% when the labeled reference was a 2-h-induced lysate (Fig. 6*A*, compare the last two columns). Similar displacement values were obtained by following the behavior of RNAP in 1- and 2-h-induced cells, again using anti-αRNAP mAb for detection. However, no differential expression of RNAP was observed in cells when βRNAP/anti-βRNAP mAb or β'RNAP/anti-β'RNAP mAb couples were used for detection. The failure to detect the RNAP displacement with anti-β'RNAP mAbs was not related to small differences in the amount of 1- and 2-h-induced lysates (see Fig. 5) because negative results were also obtained with mixtures of 1- and 5-h-induced cell lysates (data not shown).

To find out whether profiling of RNAP can be detected on anti-βRNAP or anti-β'RNAP arrayed mAbs by the alternative two-color fluorescence method, we mixed lysates from *E. coli* BL21Star (DE3) (pET duet1 his-rpoA, rpoB/pACYC duet1 rpoC, rpoZ) cells induced for 1 h or 5 h and labeled, respectively, with Alexa Fluor 680 and IRDye 800CW. As shown in Fig. 6*B*, greater RNAP expression was detected in 5-h-induced cells *versus* 1-h-induced cells following anti-β'RNAP mAb (NMRAT of 1.54) and anti-αRNAP mAb (NMRAT of 1.30) with 95% statistical confidence, whereas no difference was

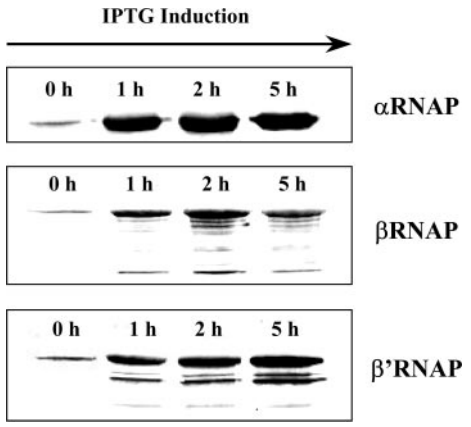

FIG. 5. **Expression of RNAP subunits in recombinant *E. coli*.** Western blot of RNAP α, β, and β' subunits synthesized in noninduced (0 h) and IPTG-induced (1–5 h) *E. coli* BL21Star (DE3) (pET duet1 rpoA, rpoB/pACYC duet1 rpoC, rpoZ) strain.

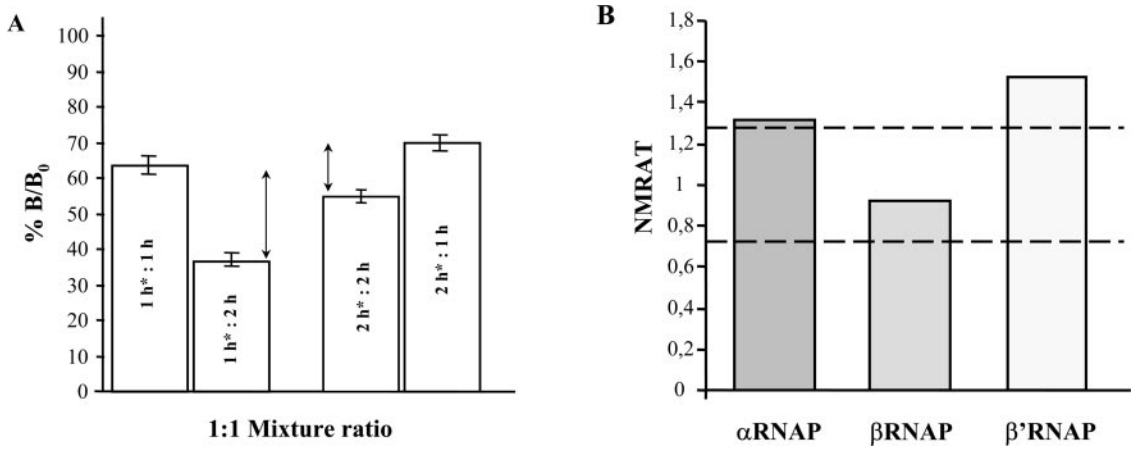

FIG. 6. **Comparison of RNAP "profiling" in bacterial lysates with one-color and two-color fluorescence detection.** *A*, one-color detection. Displacement of labeled lysates of 1-h-induced by unlabeled 1-h-induced (1 h*:1 h) or by unlabeled 2-h-induced (1 h*:2 h) lysates of *E. coli* BL21Star (DE3) (pET rpoA-his) cells, and 2-h-induced by unlabeled 2-h-induced (2 h*:2 h) or by unlabeled 1-h-induced (2 h*:1 h) lysates of *E. coli* BL21Star (DE3) (pET rpoA-his) cells. *B*, competition between two fluorescence dye labeled lysates of 1-h- and 5-h-induced *E. coli* BL21Star (DE3) (pET duet1 rpoA, rpoB/pACYC duet1 rpoC, rpoZ) strains was assessed with anti-αRNAP, anti-βRNAP, and anti-β'RNAP mAbs.

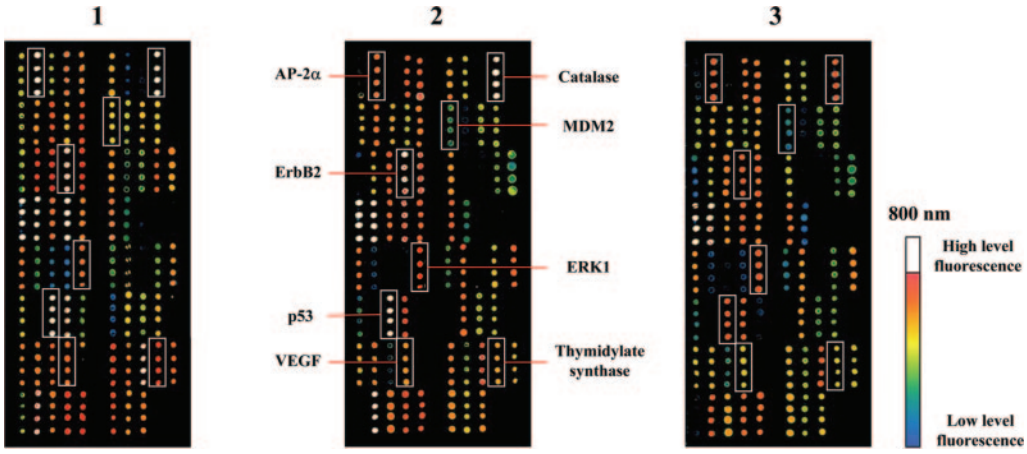

FIG. 7. **Protein profiling in breast tumor-derived lines by one-color detection.** *Slide 1*, reference array incubated with MDA MB-231 lysate alone labeled with IRDye 800CW; *slide 2*, labeled MDA MB-231 lysate mixed at a 1:1 ratio with unlabeled MDA MB-231 lysate; *slide 3*, labeled MDA MB-231 lysate mixed at a 1:1 ratio with unlabeled SKBR3 lysate. Spots corresponding to antibodies against proteins found to be overexpressed in SKBR3 cells are indicated.

observed with the anti-βRNAP mAb as it had an NMRAT value of 0.93, which is in the range of 0.72–1.28 (see "Experimental Procedures").

Comparative Protein Profiling in Breast Cancer Cells by One-color and Two-color Detection—Given the data obtained with "profiling" bacterial RNAP, we used one-color and two-color methods to evaluate their performance in assessing the differential expression of numerous proteins in breast cancer cell lines. An array of 72 selected antibodies was prepared by spotting each antibody in quadruplicate on FAST slides.

First, we compared the competitive displacement of labeled total proteins from MDA MB-231 cell lysates by unlabeled proteins from the same lysate. A decrease in fluorescence intensity was observed for many spots when mixing the two lysates at 1:1 and 1:10 ratios as compared with the reference array bound labeled lysate alone (Fig. 7, slides 1 and 2, and data not shown). We used data from the most informative 28 antibodies that gave the highest signals and analyzed the displacement characteristics at two ratios of mixed lysates. The expected theoretical values of ~50 and ~90% fluorescence diminution were detected for only 10 and 8 mAbs, respectively, whereas others gave significant deviations from the expected displacement values.

Next, we mixed labeled lysate from MDA MB-231 cells with unlabeled lysate from SKBR3 cells at 1:1 and 1:10 ratios and evaluated the competitive displacement between proteins from the two cell lines (Fig. 7 and data not shown). The difference in fluorescence intensity displayed as MDA MB-231 displacement minus SKBR3 displacement and showed increased abundance of AP-2α, VEGF, p53, ErbB2, catalase, MDM2, thymidylate synthase, and ERK1 proteins in SKBR3 cells.

In a parallel assay with the same antibody array, total proteins from the MDA MB-231 and SKBR3 cell lines were analyzed by two-color fluorescence detection (Fig. 8). Seven proteins, AP-2α, cyclin D_3, cyclin E, thymidylate synthase, catalase, 14.3.3σ, and ErbB2, were found to be more abundant in SKBR3 cells than in MDA MB-231 cells with 70% statistical confidence. Moreover, even at the more stringent 90% statistical confidence level, 14.3.3σ and ErbB2 were still found to be up-regulated in SKBR3 cells.

Higher abundance was confirmed for five proteins, AP-2α, cyclin E, catalase, 14.3.3σ, and ErbB2, in SKBR3 cells by Western blot analysis (see Fig. 8). In contradiction of the one-color results, weaker bands were detected for MDM2 (data not shown) and p53 proteins in SKBR3 cells compared with MDA MB-231, in agreement with previous data (26). We did not detect bound bands for cyclin D_3 or thymidylate synthase, which may be explained either by too low abundance to be detected by Western blot or by their degradation during storage. Two control proteins, ERK1 and β-actin, which are known to be synthesized at equal levels in the both cell lines (27, 28), showed bands of almost identical intensity in the corresponding lysates.

These data indicated that both the one-color and two-color methods detected differential expression of the same four proteins, AP-2α, catalase, thymidylate synthase, and ErbB2. However, overall two-color detection was more reliable than the one-color method in terms of its capacity to evaluate precise differential expression of a greater number of proteins in cells under the conditions used.

Improving Protein Profiling with Enriched Nuclear Proteins Using the Two-color Method—Analysis of NMRAT values indicated that some nuclear proteins showed a tendency toward differential expression with 60% statistical confidence when total protein lysates were used for profiling with the two-color method. Assuming that nuclear proteins are underrepresented in our total cellular lysates, we wondered whether the profiling performance could be improved using an enriched nuclear subfraction.

We therefore performed similar experiments with nuclear

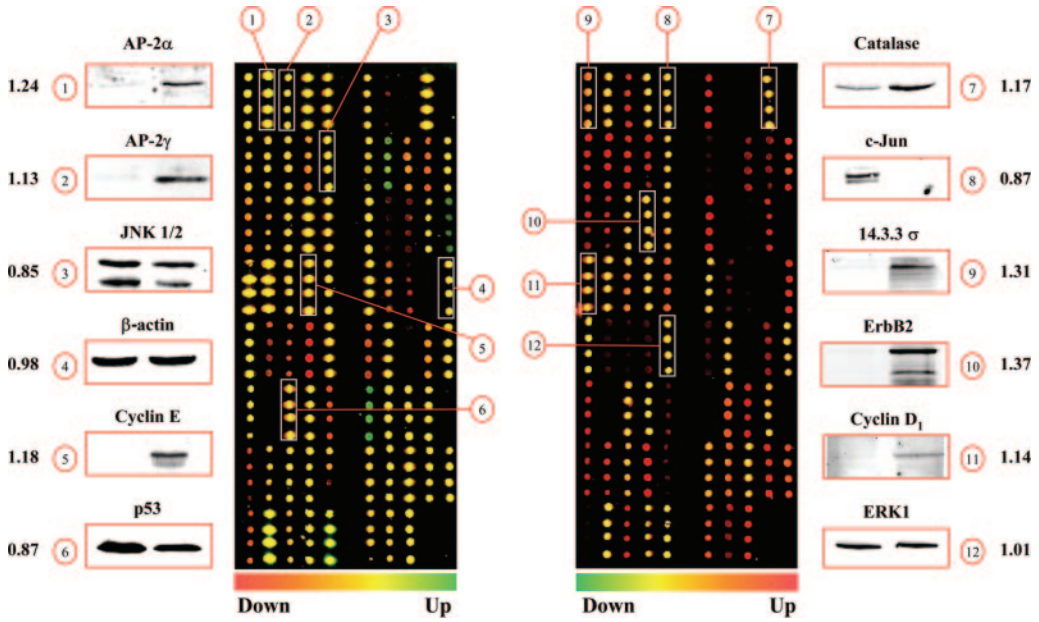

FIG. 8. **Two-color protein profiling in cell lysates from breast tumor lines.** *Left-hand array*, IRDye 800CW (*red*)-labeled MDA MB-231 lysate *versus* Alexa Fluor 680 (*green*)-labeled SKBR3; *right-hand array*, IRDye 800CW-labeled SKBR3 lysate *versus* Alexa Fluor 680-labeled MDA MB-231. Western blots: *left lane*, lysate from MDA MB-231 cells; *right lane*, lysate from SKBR3 cells. *Circled numbers* refer to position in the array of antibodies used in the corresponding Western blot; *numbers* in *bold* beside Western blot correspond to NMRAT values. Statistical confidences corresponding to each cutoff level are presented in "Experimental Procedures."

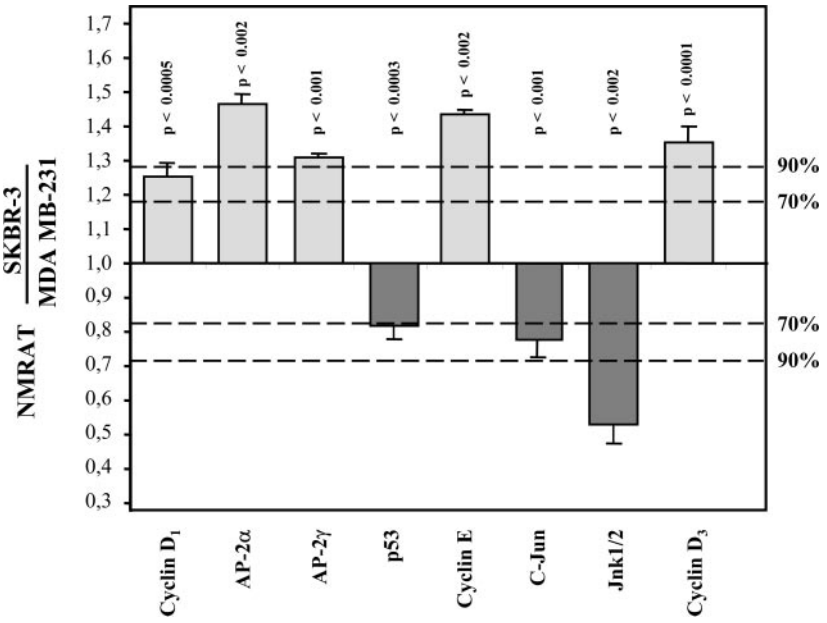

FIG. 9. **Differential expression of proteins in breast cancer cell lines using nuclear extracts.** Graph showing a compilation of data from three two-color profiling experiments performed independently. *P* was calculated for each target protein using ANOVA. Seventy and 90% represent the statistical confidence for the proteins with NMRAT values outside the cutoff levels of 0.82–1.18 and 0.71–1.29, respectively.

extracts from MDA MB-231 and SKBR3 cell lines followed by two-color fluorescence detection. Eight proteins were found to be differentially expressed. Cyclin D_1, AP-2α, AP-2γ, cyclin E, and cyclin D_3 were expressed at higher levels in SKBR3 cells, whereas p53, c-Jun, and JNK1/2 were reduced in the same cells with 70% statistical confidence (Fig. 9). The remarkable differential expression of AP-2α, cyclin E, cyclin D_3, AP-2γ, and JNK1/2 was further validated using a more stringent NMRAT interval of 0.71–1.29 corresponding to 90% statistical confidence. Western blotting of total protein from MDA MB-231 and SKBR3 cells confirmed that cyclin D_1 and AP-2γ were overexpressed in SKBR3 cells, whereas c-Jun and JNK1/2 were at a lower abundance in these cells (see Fig. 8). The presence of two bands for JNK1/2 is due to recognition of the same epitope on two related JNK proteins by the anti-JNK1/2 mAb. These data confirmed that nuclear protein

subfractionation provides more precise profiling information about the nuclear proteome in these cells.

DISCUSSION

High throughput protein profiling allows the measurement of the relative concentration of numerous target molecules in two analytes using a single binding assay with immobilized antibodies. Two different evaluations based on the competition principle, termed one-color and two-color detection, have been proposed to study protein profiling in human cells and tissues. Considering the potential advantages of one-color detection (14), we have performed a detailed competitive displacement study of selected target proteins, presented as single- or multi-subunit complex molecules, to evaluate fully the strengths and weaknesses of this method.

A model protocol, composed of mAbs immobilized on an NC membrane probed with bacterial RNA polymerase subunits and analytes containing purified or nonpurified target proteins, showed that one-color detection provides an accurate assessment of the competitiveness of αRNAP or RNAP, when displacement is determined with an anti-αRNAP mAb. In contrast, no displacement of RNAP could be detected using anti-β'RNAP mAbs with the one-color method, whereas this was possible with the same mAb using the two-color evaluation. How can this discrepancy be explained?

Random conjugation of almost 1 kDa of fluorescent dyes to the reference protein (2–3 dye molecules/protein) increases not only a protein's molecular mass, but also affects its folding, solubility, migration, and molecular recognition properties. As a consequence, the competitiveness of labeled proteins can be dramatically changed with respect to unlabeled ones when evaluated by one-color detection. In contrast, in two-color evaluation, both protein samples are labeled by chemically similar dyes through amine-reactive NHS ester bonds of the IRDyes. Even if physico-chemical properties are disrupted in the labeled proteins, the two samples remain highly similar to each other and hence are likely to display similar competition activity for the antibody, and thus the displacement better reflects protein expression differences in mixed analytes. Moreover, running two binding assays in parallel with mutually exchanged dyes results in, after normalization, a significant decrease in interference from dye conjugation bias.

These conclusions were born out when we profiled complex protein mixtures in breast cancer cell lysates using the two detection methods. The expression profile determined for several proteins using the one-color method was not confirmed by Western blot. However, the two-color method detected modulations in the level of expression of proteins that were not revealed using one-color detection. Therefore, we conclude that two-color profiling extends the utility of fluorescent assessment to a larger number of target proteins and is clearly better suited to high throughput analysis of differential expression of complex proteomes from mammalian cells.

The specificity of antigen-antibody interaction is a function of their affinity and antibody cross-reactivity, and this takes on a special significance in protein profiling studies (29–31). Indeed, we have found that data obtained from some spots are impossible to interpret because of the high cross-reactivity of the antibodies as revealed by subsequent Western blot analysis. In addition, this study raises other important issues that can be useful for further improving the performance of high throughput protein profiling with array technology.

Western blot analysis has shown that anti-βRNAP and anti-β'RNAP mAbs bind to many smaller-molecular-mass species that accumulated in lysates from IPTG-induced cells (see Fig. 5). Such a pool of truncated β and β' subunits can interfere with the competitive displacement of whole RNAP assembled from full-length subunits. Notably, truncated derivatives were also observed for overexpressed cyclin E, 14.3.3σ, and ErbB2 in SKBR3 as well as for c-Jun in MDA MB-231 breast cancer cells. Therefore, we suggest that the presence of truncated proteins will contribute to a diminution in the specificity of antigen-antibody interactions and can thereby disrupt protein profiling performance.

We have also shown that the assessment of RNA polymerase expression depends strongly on the accessibility of the target epitopes by anti-subunit mAbs. Neither of the two methods detected variations in RNAP expression when competition was monitored by β subunit binding to the anti-βRNAP mAb. In agreement with this observation, the affinity purification of *E. coli* RNA polymerase using anti-βRNAP mAb has been found to be inefficient in comparison with anti-αRNAP and anti-β'RNAP mAbs (32, 33). The three-dimensional structure of the related *Thermus thermophilus* RNA polymerase is available (34) and suggests a logical explanation for these negative results. It turns out that the β epitope is almost completely masked by the other subunits, whereas the epitopes in the two α and β' subunits are exposed on the surface of the RNAP holoenzyme (see Fig. 1*A*). As many proteins are organized into multi-molecular complexes in eukaryotic cells, we speculate that the efficiency of profiling proteins in their native state will be heavily influenced by the usually unpredictable accessibility of antibody recognition sites.

Low protein abundance is another limiting factor for protein profiling on minute planar spot surfaces when a total protein lysate is used. Near-infrared fluorescence allows the detection of attomol quantities of target molecules without signal amplification from protein patterns immobilized on a porous nitrocellulose support (21) with a sensitivity that is comparable to tyramide amplification and sufficient to assess the phosphorylation state in arrayed total proteins extracted from cancer biopsies (35). Unfortunately, the low proportion of target molecules in total protein lysates, used as solution analyte or as a printed analyte, strongly restricts the number of molecules that can be captured by the antibodies and thence be detected by near-infrared fluorescence. This limitation cannot be overridden by increasing the analyte concentration due to

spot saturation. However, an analyte, enriched by target proteins isolated from the nucleus, can allow the identification of differential nuclear expression patterns that would not be detected using a total lysate. It appears that the use of a compartment-specific fraction provides both an augmentation in the proportion of target molecules in the analyte and a diminution in antibody cross-reactivity toward nontarget molecules located in other cellular compartments. Both aspects are crucial to increase the specificity of antigen recognition and the sensitivity of protein profiling.

A major advantage of antibody array technology is the protein profiling of tumors in a single experiment. Here, 12 proteins have been identified as increased or decreased in expression in two breast cancer cell lines, SKBR3 *versus* MDA MB-231, using a microarray prepared from 72 selected antibodies. Similar data obtained by other methods confirm these results for AP-2α and AP-2γ (36), ErbB2 (37, 38), p53 (26), and c-Jun (37). A clear modulation of seven more proteins, including three cyclins D_1, D_3, and E, JNK1/2, thymidylate synthase, catalase, and 14.3.3σ, underlies a wider pleiotropic effect of the cancer mutation(s) in the two cell lines.

The correlation between high levels of the AP-2α and AP-2γ DNA binding transcription factors with overexpression of the *ERBB2* proto-oncogene in tumor-derived cell lines has been documented previously (36). The antibody array data presented here were able to confirm this functional linkage by detecting the up-regulation of the AP-2 factors in ErbB2-positive SKBR3 cells *versus* ErbB2-negative MDA MB-231 cells, particularly when protein lysates enriched for nuclear factors were employed (see Fig. 9). This provides an important validation of our methodology and supports the possibility of being able to derive biological information by comparing the proteomes of other tumor-derived cell lines and ultimately tumor samples, and this is now under investigation.

We have also used our current data to compare more narrowly the biology of the two cell lines used in this study. Although not phenotypically alike, the two breast tumor-derived cell lines compared in this study share several features characteristic of poor prognosis breast cancer patients. Both lines are negative for the estrogen receptor and also carry mutations in their p53 genes. Moreover, the MDA MB-231 line is noted for carrying an activated *Ha-Ras* gene, and SKBR3 cells are extensively studied due to the amplification of their *ERBB2(neu)* gene, which contributes to the overexpression of this receptor, as noted above (see Fig. 8). In breast epithelial cells, ErbB2 lies upstream of Ras in the mitogenic signaling pathway (39), which leads to transcriptional induction of cyclin D_1 (40, 41). Furthermore, activation of cyclin D_1 by this pathway is essential in this cell type as demonstrated by studies in cyclin D_1 null mice that are resistant to mammary carcinogenesis induced by either *ras* or *neu* oncogenes (42). By complexing with their partner kinases Cdk4/6 and Cdk2 to induce progressive phosphorylation and inactivation of pRb, the D-type and E-type cyclins control G_1 to S phase transition during normal cell-cycle progression. Therefore, as both MDA MB-231 and SKBR3 cells are activated in essentially the same pathway and both have an intact *RB* gene, the levels of expression of these key growth factor target genes might be expected to be similar in the two cell lines. In our proteomic study, however, we find clear increased levels of cyclins D_1, D_3, and E in SKBR3 cells compared with the MDA MB-231 line, particularly when nuclear extracts are compared (see Fig. 9). Previous comparison of these lines at the RNA level had not indicated these differences in expression level (43). This suggests therefore that for mitogenic cyclins, post-transcriptional regulation of their protein levels is important.

Given the apparently mammary-specific wiring of the *ERBB2/neu*-Ras-cyclin D_1 pathway, it has been argued that an anti-cyclin D_1 therapy would be optimal for patients overexpressing ErbB2 (42). However, elevated cyclin E (both full-length and low-molecular-mass forms) has also been associated with poor survival in this disease and in multivariate analysis was more closely associated with outcome than levels of cyclin D_1, D_3, or ErbB2 (44). Moreover, because cyclin E acts downstream of cyclin D_1, cells and tumors expressing even slightly elevated levels may bypass therapies targeted to cyclin D_1 alone. The subtle differences, highlighted here, between two lines activated in the same signaling pathway could therefore prove to be a useful model system to test the efficacy of such therapies.

The data presented here show that NC-prepared microarrays provide repetitive and precise measurements of antigen-antibody interactions through protein competition for corresponding antibodies using both eukaryotic and prokaryotic lysates. We have recently demonstrated the possibility of an accurate comparative assessment of the antibody binding affinity of IgG purified from the sera of AIDS patients using a panel of arrayed phage-displayed peptides (19). Together, these data are encouraging in terms of the development of reliable immunoassays to assess binding parameters of complex protein mixtures within a range of the sensitivity useful for biomedical investigations and applications.

Acknowledgment—We thank Gabriel Ricolleau for discussions.

* This study was supported by the "Post-Génome" program (Contrat Etat Région des Pays de la Loire). G. Y. and G. L. are postgraduate students supported respectively by the National Council for Scientific Research Lebanon (CNRSL) and Ministère de la Recherche (ANRT)/ProtNeteomix. The costs of publication of this article were defrayed in part by the payment of page charges. This article must therefore be hereby marked "*advertisement*" in accordance with 18 U.S.C. Section 1734 solely to indicate this fact.

‖ To whom correspondence should be addressed: Biotechnologie, Biocatalyse, Biorégulation, Unité Mixte de Recherche 6204, Centre National de la Recherche Scientifique, Université de Nantes, 2 rue de la Houssinière, 44322 Nantes, France. Tel.: 33-251125620; Fax: 33-251125637; E-mail: Vehary.Sakanyan@chimbio.univ-nantes.fr, v.sakanyan@protneteomix.com.

REFERENCES

1. Ekins, R., and Chu, F. (2003) In *Protein Arrays, Biochips, and Proteomics. The Next Phase of Genomic Discovery* (Albala, J. S., and Humphery-Smith, I., eds) Ultrasensitive Microarray-Based Ligand Assay Technology, pp. 81–125, Marcel Dekker, Inc., New York
2. Kodadek, T. (2001) Protein microarrays: Prospects and problems. *Chem. Biol.* **8,** 105–115
3. Sreekumar, A., Nyati, M. K., Varambally, S., Barrette, T. R., Ghosh, D., Lawrence, T. S., and Chinnaiyan, A. M. (2001) Profiling of cancer cells using protein microarrays: Discovery of novel radiation-regulated proteins. *Cancer Res.* **61,** 7585–7593
4. Haab, B. B., Dunham, M. J., and Brown, P. O. (2001) Protein microarrays for highly parallel detection and quantitation of specific proteins and antibodies in complex solutions. *Genome Biol.* **2,** RESEARCH0004
5. Knezevic, V., Leethanakul, C., Bichsel, V. E., Worth, J. M., Prabhu, V. V., Gutkind, J. S., Liotta, L. A., Munson, P. J., Petricoin, E. F., 3rd, and Krizman, D. B. (2001) Proteomic profiling of the cancer microenvironment by antibody arrays. *Proteomics* **1,** 1271–1278
6. Huang, R. P., Huang, R., Fan, Y., and Lin, Y. (2001) Simultaneous detection of multiple cytokines from conditioned media and patient's sera by an antibody-based protein array system. *Anal. Biochem.* **294,** 55–62
7. Moody, M. D., Van Arsdell, S. W., Murphy, K. P., Orencole, S. F., and Burns, C. (2001) Array-based ELISAs for high-throughput analysis of human cytokines. *BioTechniques* **31,** 186–190, 192–194
8. Schweitzer, B., Roberts, S., Grimwade, B., Shao, W., Wang, M., Fu, Q., Shu, Q., Laroche, I., Zhou, Z., Tchernev, V. T., Christiansen, J., Velleca, M., and Kingsmore, S. F. (2002) Multiplexed protein profiling on microarrays by rolling-circle amplification. *Nat. Biotechnol.* **20,** 359–365
9. Tam, S. W., Wiese, R., Lee, S., Gilmore, J., and Kumble, K. D. (2002) Simultaneous analysis of eight human Th1/Th2 cytokines using microarrays. *J. Immunol. Methods* **261,** 157–165
10. Tannapfel, A., Anhalt, K., Hausermann, P., Sommerer, F., Benicke, M., Uhlmann, D., Witzigmann, H., Hauss, J., and Wittekind, C. (2003) Identification of novel proteins associated with hepatocellular carcinomas using protein microarrays. *J. Pathol.* **201,** 238–249
11. Miller, J. C., Zhou, H., Kwekel, J., Cavallo, R., Burke, J., Butler, E. B., Teh, B. S., and Haab, B. B. (2003) Antibody microarray profiling of human prostate cancer sera: Antibody screening and identification of potential biomarkers. *Proteomics* **3,** 56–63
12. Nielsen, U. B., Cardone, M. H., Sinskey, A. J., MacBeath, G., and Sorger, P. K. (2003) Profiling receptor tyrosine kinase activation by using Ab microarrays. *Proc. Natl. Acad. Sci. U. S. A.* **100,** 9330–9335
13. Zhou, H., Bouwman, K., Schotanus, M., Verweij, C., Marrero, J. A., Dillon, D., Costa, J., Lizardi, P., and Haab, B. B. (2004) Two-color, rolling-circle amplification on antibody microarrays for sensitive, multiplexed serum-protein measurements. *Genome. Biol.* **5,** R28
14. Barry, R., Diggle, T., Terrett, J., and Soloviev, M. (2003) Competitive assay formats for high-throughput affinity arrays. *J. Biomol. Screen.* **8,** 257–263
15. Barry, R., and Soloviev, M. (2004) Quantitative protein profiling using antibody arrays. *Proteomics* **4,** 3717–3726
16. Kimura, M., and Ishihama, A. (1996) Subunit assembly *in vivo* of *Escherichia coli* RNA polymerase: Role of the amino-terminal assembly domain of α subunit. *Genes Cells* **1,** 517–528
17. Schutz, A. R., Altschuler, Y., Mostov, K. E., and Olive, D. M. (2000). Highly sensitive detection of proteins on membranes with near-infrared fluorescence. Available on-line at www.licor.com
18. Ghochikyan, A., Karaivanova, I. M., Lecocq, M., Vusio, P., Arnaud, M. C., Snapyan, M., Weigel, P., Guevel, L., Buckle, M., and Sakanyan, V. (2002) Arginine operator binding by heterologous and chimeric ArgR repressors from *Escherichia coli* and *Bacillus stearothermophilus*. *J. Bacteriol.* **184,** 6602–6614
19. Arnaud, M. C., Gazarian, T., Rodriguez, Y. P., Gazarian, K., and Sakanyan, V. (2004) Array assessment of phage-displayed peptide mimics of human immunodeficiency virus type 1 gp41 immunodominant epitope: Binding to antibodies of infected individuals. *Proteomics* **4,** 1959–1964
20. Saghatelyan, A. K., Snapyan, M., Gorissen, S., Meigel, I., Mosbacher, J., Kaupmann, K., Bettler, B., Kornilov, A. V., Nifantiev, N. E., Sakanyan, V., Schachner, M., and Dityatev, A. (2003) Recognition molecule associated carbohydrate inhibits postsynaptic GABA(B) receptors: A mechanism for homeostatic regulation of GABA release in perisomatic synapses. *Mol. Cell. Neurosci.* **24,** 271–282
21. Snapyan, M., Lecocq, M., Guevel, L., Arnaud, M. C., Ghochikyan, A., and Sakanyan, V. (2003) Dissecting DNA-protein and protein-protein interactions involved in bacterial transcriptional regulation by a sensitive protein array method combining a near-infrared fluorescence detection. *Proteomics* **3,** 647–657
22. Smith, P. K., Krohn, R. I., Hermanson, G. T., Mallia, A. K., Gartner, F. H., Provenzano, M. D., Fujimoto, E. K., Goeke, N. M., Olson, B. J., and Klenk, D. C. (1985) Measurement of protein using bicinchoninic acid. *Anal. Biochem.* **150,** 76–85
23. Bradford, M. M. (1976) A rapid and sensitive method for the quantitation of microgram quantities of protein utilizing the principle of protein-dye binding. *Anal. Biochem.* **72,** 248–254
24. Eloranta, J. J., and Hurst, H. C. (2002) Transcription factor AP-2 interacts with the SUMO-conjugating enzyme UBC9 and is sumolated *in vivo*. *J. Biol. Chem.* **277,** 30798–30804
25. Rodbard, D. (1974) Statistical quality control and routine data processing for radioimmunoassays and immunoradiometric assays. *Clin. Chem.* **20,** 1255–1270
26. Phelps, M., Darley, M., Primrose, J. N., and Blaydes, J. P. (2003) p53-independent activation of the hdm2-P2 promoter through multiple transcription factor response elements results in elevated hdm2 expression in estrogen receptor α-positive breast cancer cells. *Cancer Res.* **63,** 2616–2623
27. Filardo, E. J., Quinn, J. A., Bland, K. I., and Frackelton, A. R., Jr. (2000) Estrogen-induced activation of Erk-1 and Erk-2 requires the G protein-coupled receptor homolog, GPR30, and occurs via trans-activation of the epidermal growth factor receptor through release of HB-EGF. *Mol. Endocrinol.* **14,** 1649–1660
28. Yang, X., Hao, Y., Ding, Z., Pater, A., and Tang, S. C. (1999) Differential expression of antiapoptotic gene BAG-1 in human breast normal and cancer cell lines and tissues. *Clin. Cancer Res.* **5,** 1816–1822
29. MacBeath, G. (2002) Protein microarrays and proteomics. *Nat. Genet.* **32,** (suppl.) 526–532
30. Haab, B. B. (2003) Methods and applications of antibody microarrays in cancer research. *Proteomics* **3,** 2116–2122
31. Sakanyan, V. (2004) High-throughput and multiplexed protein array technology: protein-DNA and protein-protein interactions. *J. Chrom. B* **5,** 77–95
32. Lesley, S. A., and Burgess, R. R. (1989) Characterization of the *Escherichia coli* transcription factor sigma 70: Localization of a region involved in the interaction with core RNA polymerase. *Biochemistry* **28,** 7728–7734
33. Thompson, N. E., Hager, D. A., and Burgess, R. R. (1992) Isolation and characterization of a polyol-responsive monoclonal antibody useful for gentle purification of *Escherichia coli* RNA polymerase. *Biochemistry* **31,** 7003–7008
34. Vassylyev, D. G., Sekine, S., Laptenko, O., Lee, J., Vassylyeva, M. N., Borukhov, S., and Yokoyama, S. (2002) Crystal structure of a bacterial RNA polymerase holoenzyme at 2.6 A resolution. *Nature* **417,** 712–719
35. Calvert, V. S., Tang, Y., Boveia, V., Wulfkuhle, J., Schutz-Geschwender, A., Olive, D. M., Liotta, L. A., and Petricoin, E. F. (2004) Development of multiplexed protein profiling and detection using near infrared detection of reverse-phase protein microarrays. *Clin. Proteomics* **1,** 81–90
36. Bosher, J. M., Totty, N. F., Hsuan, J. J., Williams, T., and Hurst, H. C. (1996) A family of AP-2 proteins regulates c-erbB-2 expression in mammary carcinoma. *Oncogene* **13,** 1701–1707
37. Brown, R. E. (2002) HER-2/neu-positive breast carcinoma: Molecular concomitants by proteomic analysis and their therapeutic implications. *Ann. Clin. Lab. Sci.* **32,** 12–21
38. Wu, S. L., Hancock, W. S., Goodrich, G. G., and Kunitake, S. T. (2003) An approach to the proteomic analysis of a breast cancer cell line (SKBR-3). *Proteomics* **3,** 1037–1046
39. Janes, P. W., Daly, R. J., deFazio, A., and Sutherland, R. L. (1994) Activation of the Ras signalling pathway in human breast cancer cells overexpressing erbB-2. *Oncogene* **9,** 3601–3608
40. Filmus, J., Robles, A. I., Shi, W., Wong, M. J., Colombo, L. L., and Conti, C. J. (1994) Induction of cyclin D1 overexpression by activated ras. *Oncogene* **9,** 3627–3633
41. Lee, R. J., Albanese, C., Fu, M., D'Amico, M., Lin, B., Watanabe, G., Haines, G. K. 3rd, Siegel, P. M., Hung, M. C., Yarden, Y., Horowitz, J. M., Muller,

W. J., and Pestell, R. G. (2000) Cyclin D1 is required for transformation by activated Neu and is induced through an E2F-dependent signaling pathway. *Mol. Cell. Biol.* **20,** 672–683
42. Yu, Q., Geng, Y., and Sicinski, P. (2001) Specific protection against breast cancers by cyclin D1 ablation. *Nature* **411,** 1017–1021
43. Keyomarsi, K., and Pardee, A. B. (1993) Redundant cyclin overexpression and gene amplification in breast cancer cells. *Proc. Natl. Acad. Sci. U. S. A.* **90,** 1112–1116
44. Keyomarsi, K., Tucker, S. L., Buchholz, T. A., Callister, M., Ding, Y., Hortobagyi, G. N., Bedrosian, I., Knickerbocker, C., Toyofuku, W., Lowe, M., Herliczek, T. W., and Bacus, S. S. (2002) Cyclin E and survival in patients with breast cancer. *N. Engl. J. Med.* **347,** 1566–1575